



Future Changes in Global Monsoons

ZHOU Tianjun

Thanks to: CHEN Xiaolong, ZHANG Wenxia, NANGOMBE Shingirai, YAO Junchen, ZHANG Lixia

zhoutj@lasg.iap.ac.cn

http://www.lasg.ac.cn/staff/ztj/index_e.htm

2nd WCRP Grand Challenge Meeting on Monsoons and Tropical Rain Belts

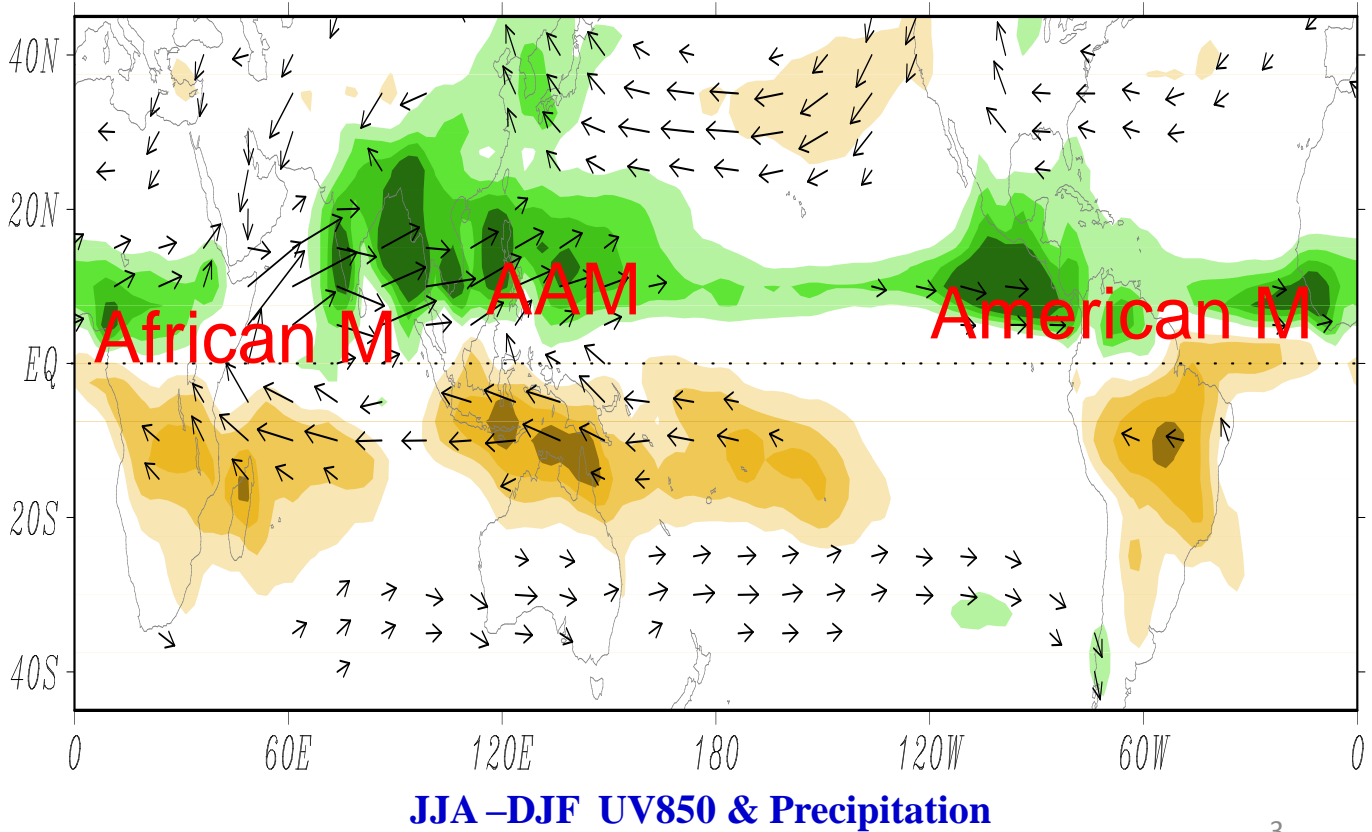


Outline

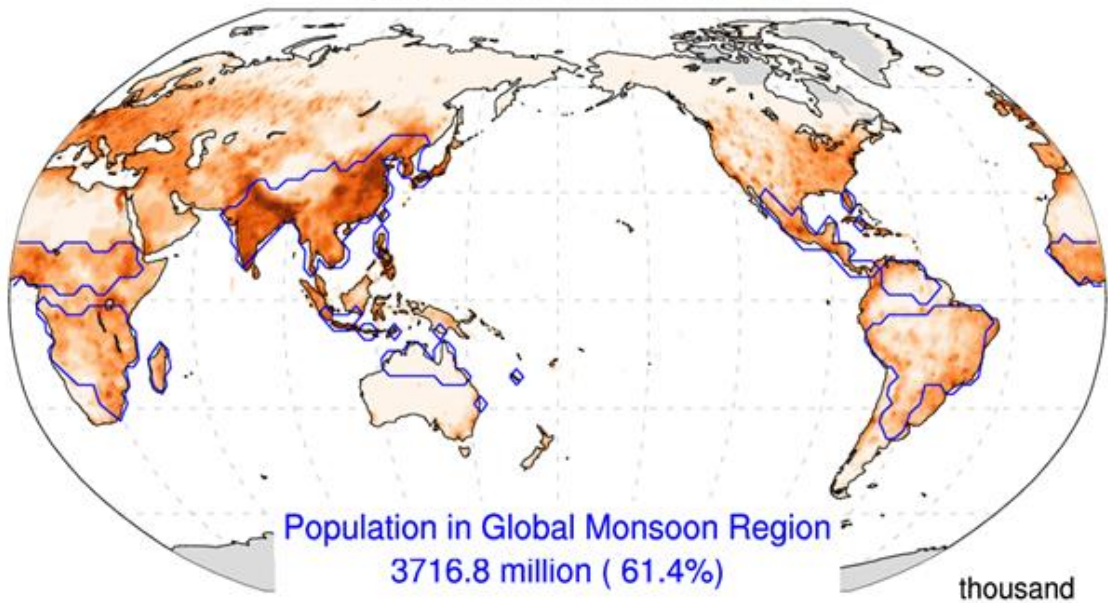
- ◆ Background: uncertainty in projection
- ◆ S. Asian monsoon: GW vs SST modulation
- ◆ E. Asian monsoon: model resolution
- ◆ Record-breaking events in Africa
- ◆ Extreme precipitation
- ◆ Summary



Global Monsoons

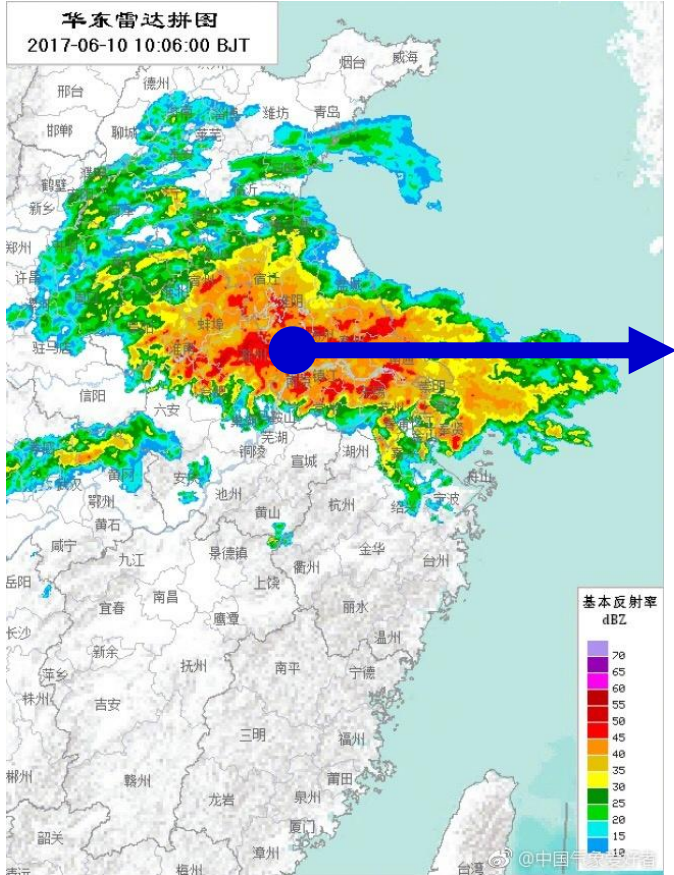


Population Counts in 2000



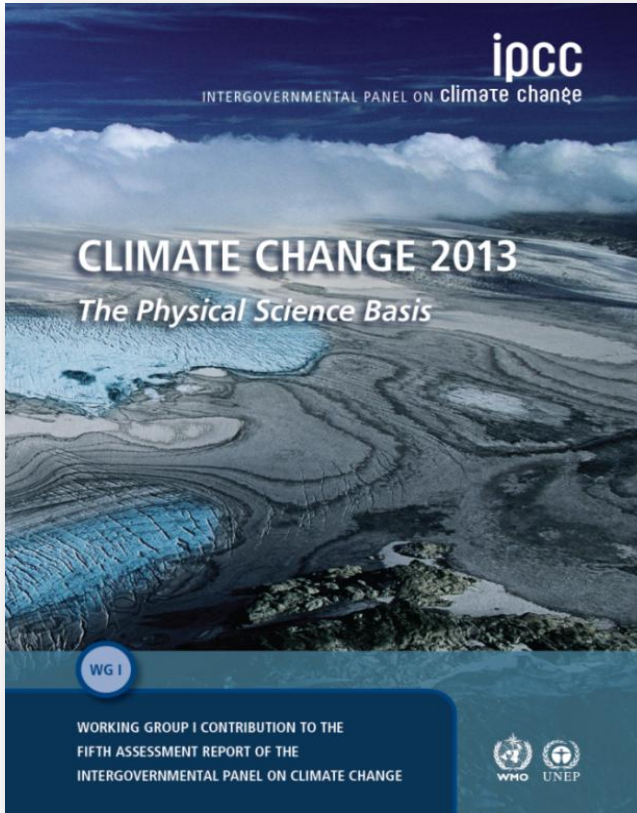
~2/3 of the population are affected by monsoon

June 10, 2017: CMA radar image, Nanjing





Monsoon Changes under Global warming

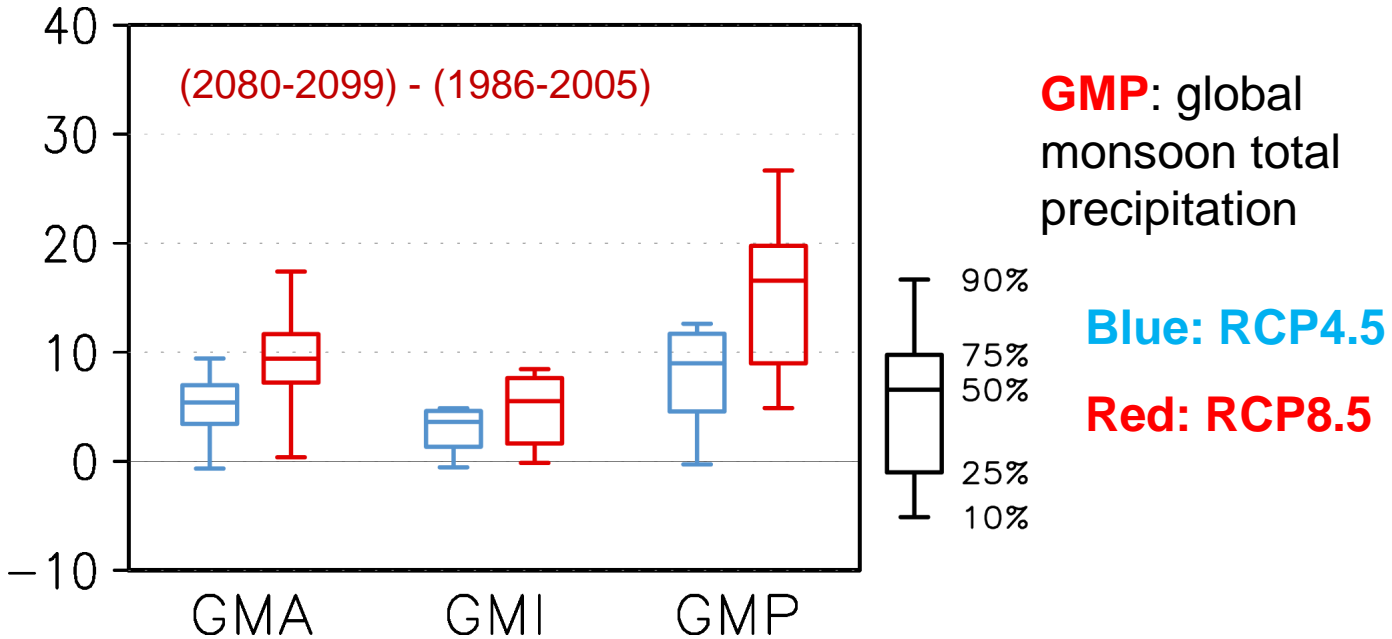


There is growing evidence of improved skill of climate models in reproducing climatological features of the global monsoon.

Taken together with identified model agreement on future changes, the global monsoon, aggregated over all monsoon systems, is likely to strengthen in the 21st century with increases in its area and intensity, while the monsoon circulation weakens.

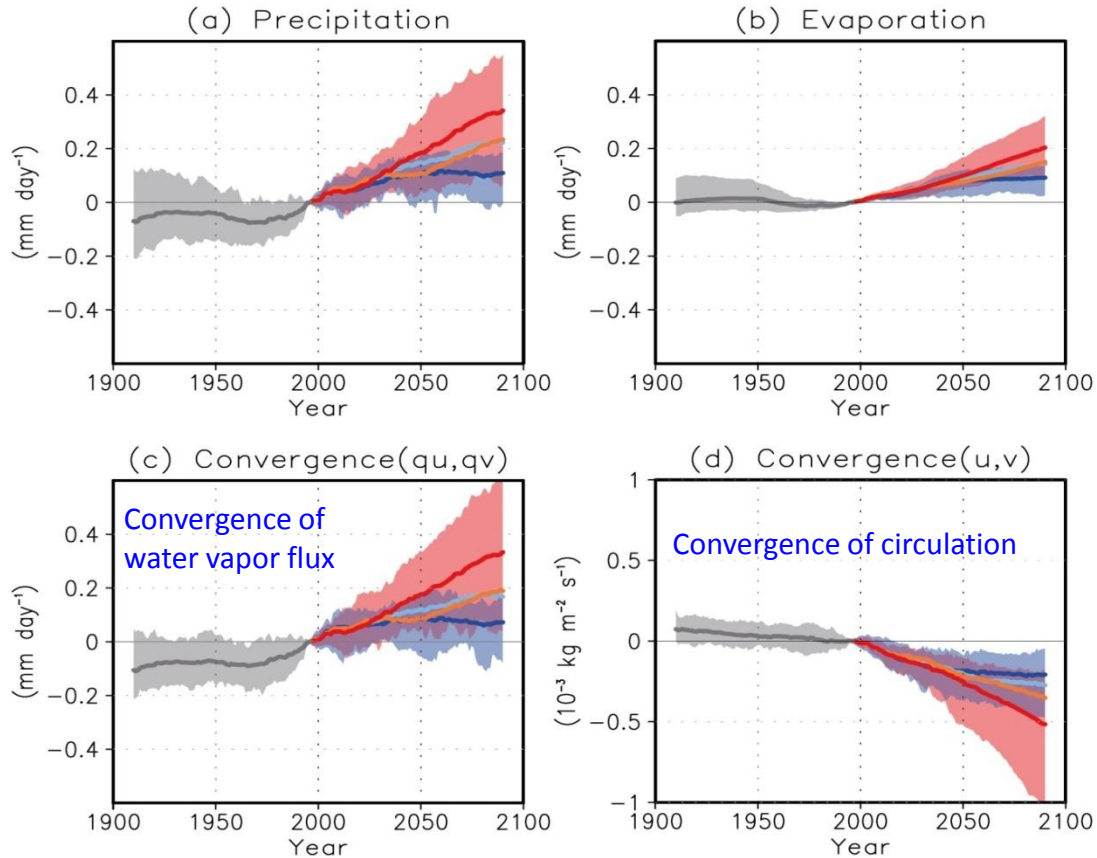
Monsoon onset dates are likely to become earlier or not to change much and monsoon retreat dates are likely to delay, resulting in lengthening of the monsoon season in many regions.

Future change (%): GMA, GMI & GMP



Monsoon-related precipitation will significantly increase in a warmer climate

An increase of moisture convergence due to increased surface evaporation and water vapor in the air column



Projected rainfall changes: regional difference and uncertainty

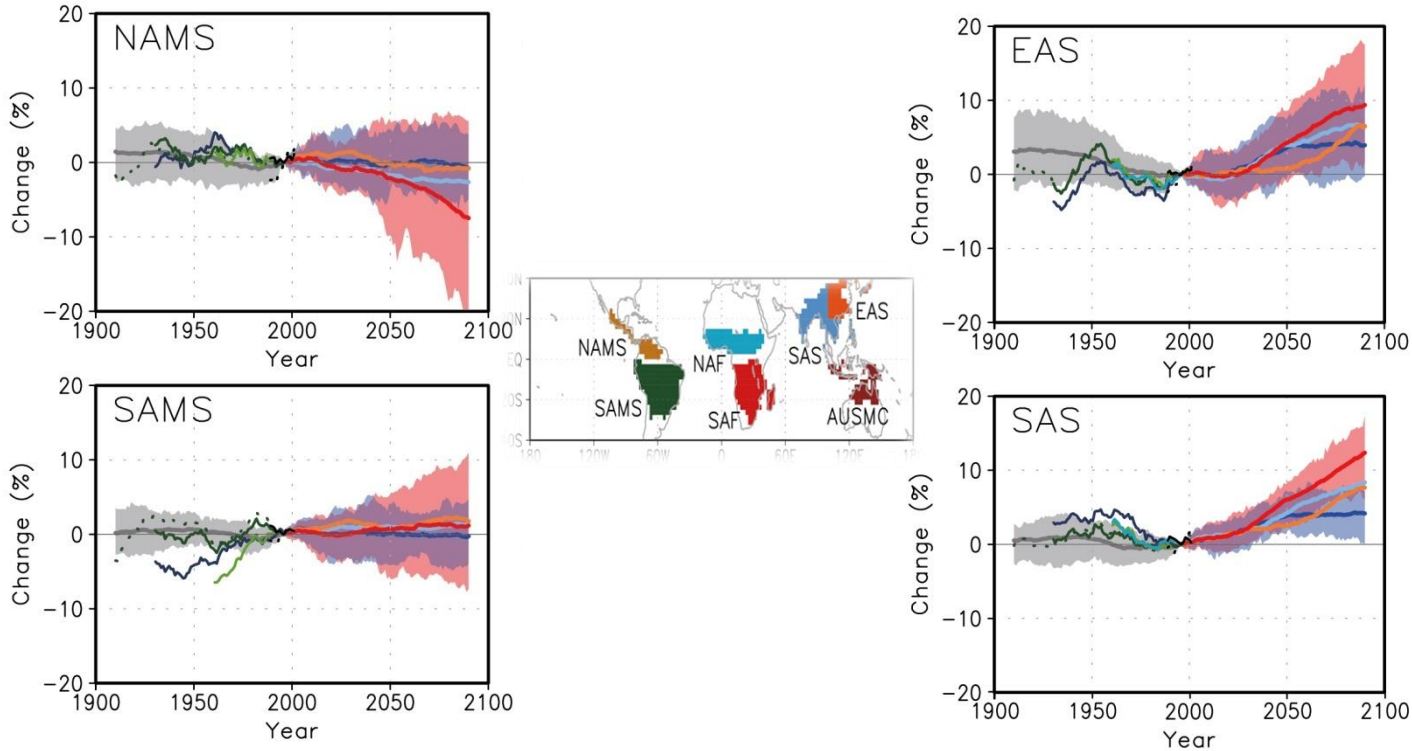
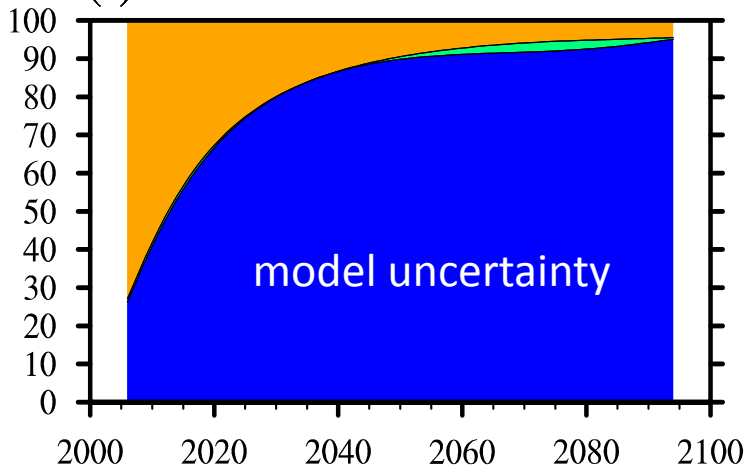


Fig.14.3, 14.4, 14.6 IPCC AR5

(a) Globe



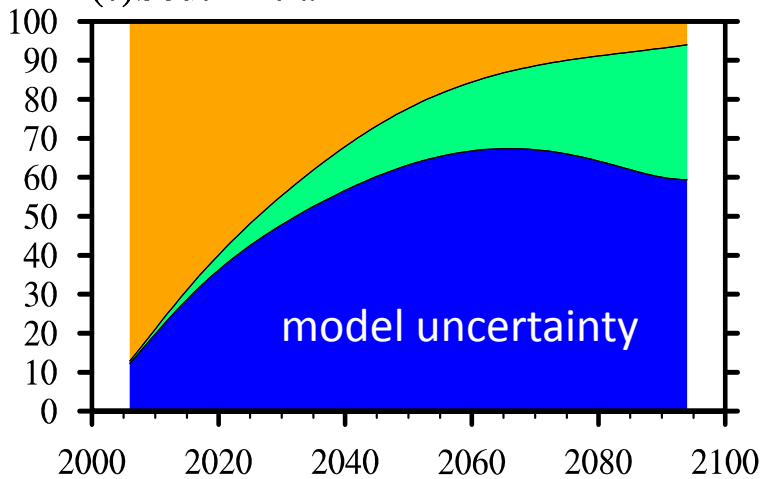
Fraction of total variance in decadal annual mean precipitation predictions **explained by the three components of total uncertainty** (relative to a 1986-2005 reference period)

Model

Scenario

Internal

(e) South Asia



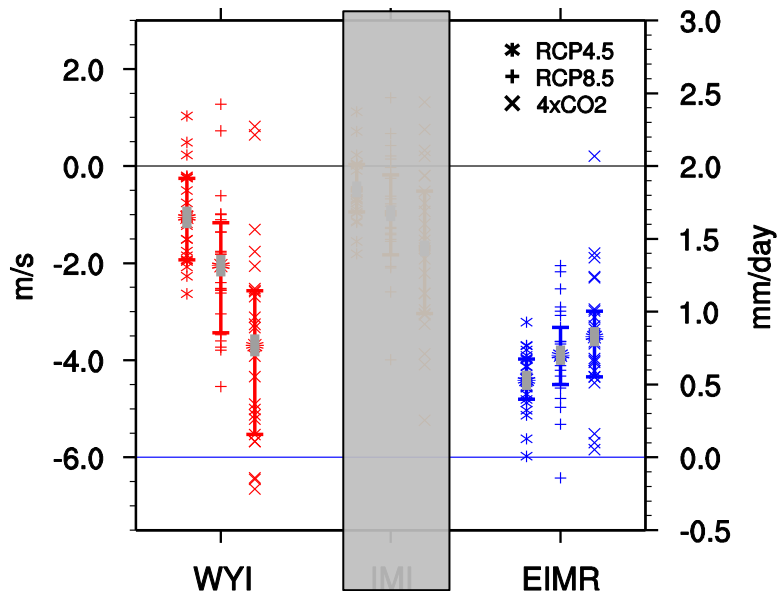
Zhou and Lu, 2018 (in preparation):
Method following *Hawkins and Sutton (2009)*

Uncertainties in **S. Asian monsoon** projection

Uncertainty in SA Monsoon Projection



Three scenario: RCP4.5, RCP8.5, 4xCO₂
Gray bar: uncertainty from internal variability

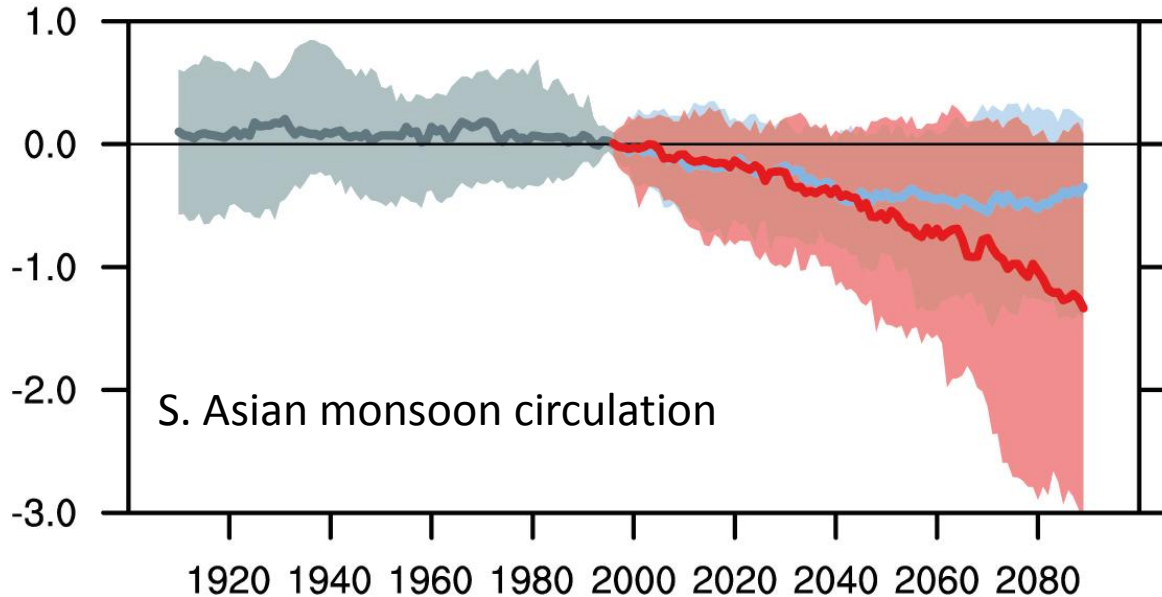


- **WYI:** Webster-Yang Index, vertical shear between 850hPa and 200hPa zonal wind
- **IMI:** Indian Monsoon Index, meridional shear of 850hPa zonal wind (vorticity, monsoon trough)
- **EIMR:** Extended Indian Monsoon Rainfall, averaged rainfall over the SASM region

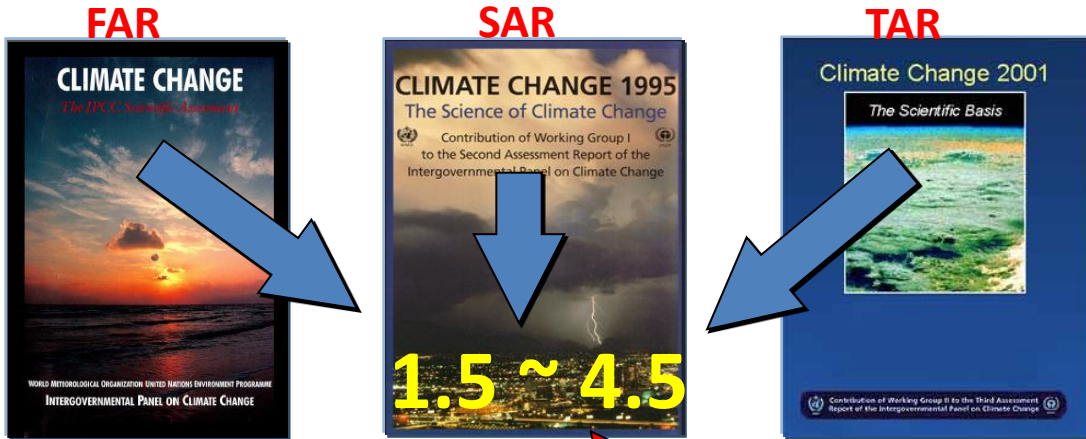
■ **Multi-model mean: Circulation weakening and rainfall increasing.**

■ **Large model spread** which cannot be explained by internal variability.

How to understand such large uncertainties in both circulation and precipitation?

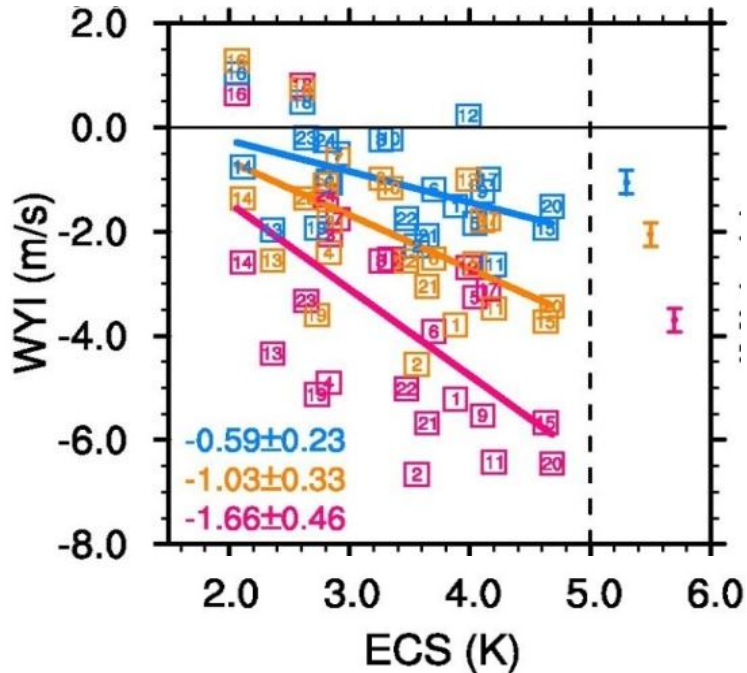


Equilibrium Climate Sensitivity: 2CO₂





WY circulation index RCP4.5 RCP8.5 4xCO₂

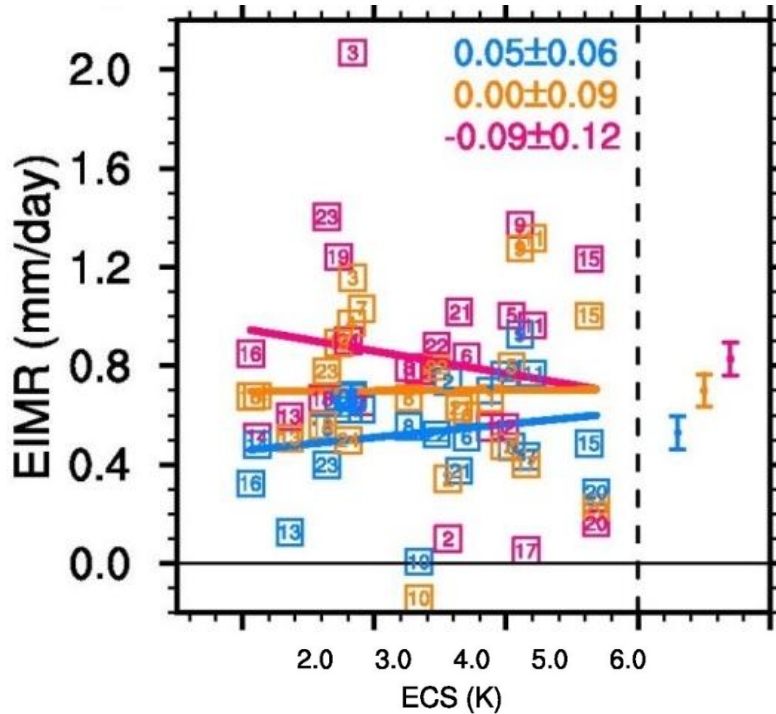


Higher ECS, weaker circulation.



Monsoon rainfall

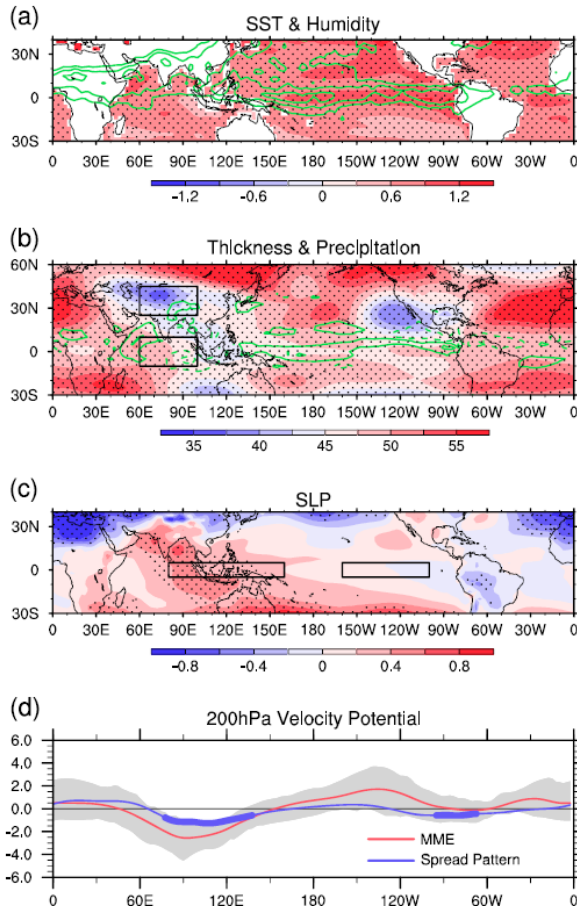
RCP4.5 RCP8.5 4xCO₂



No evident relation between ECS and SASM rainfall projection 17



Q1: Weakened monsoon circulation associated with higher ECS?



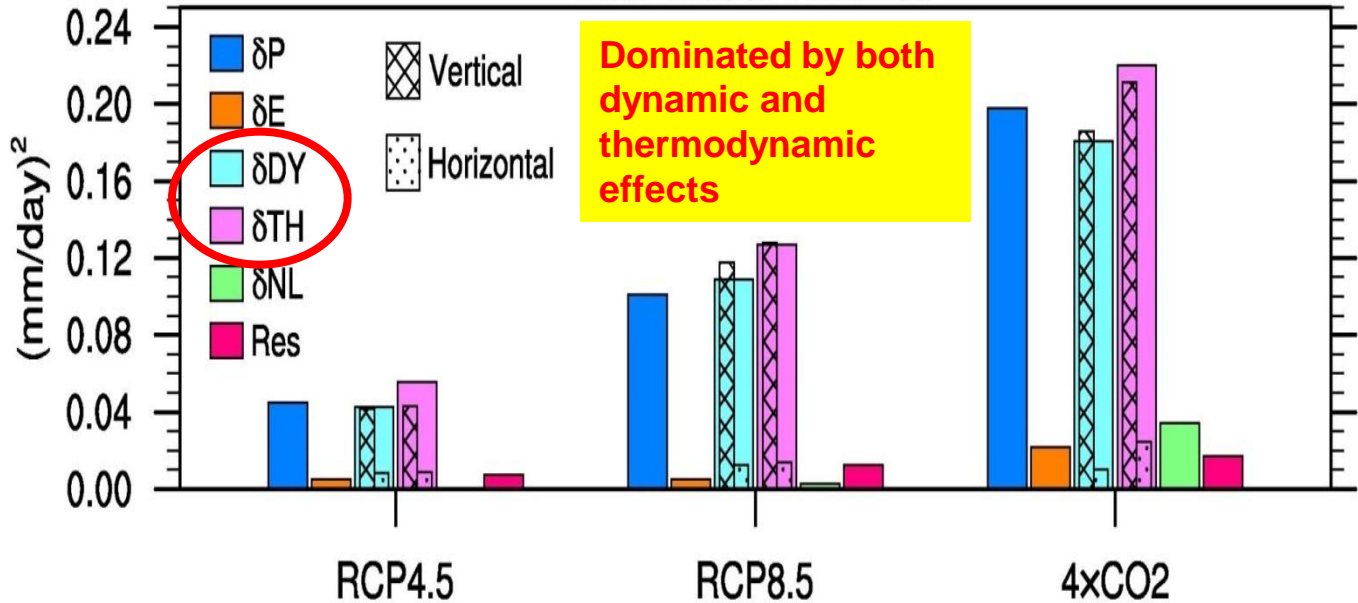
Spread pattern regressed onto GMST

- ✓ Higher climate sensitivity, warmer upper tropical troposphere (water vapor feedback)
- ✓ weaker meridional thermal contrast, weaker tropical easterly jet.
- ✓ Stronger dry static stability, weaker Walker circulation as reported previously, weaker upper level divergence over SA
- ✓ Rossby wave response to downwelling over the maritime continent -- weaker SASM trough



Q2: Rainfall Uncertainty — Moisture Budget Diagnosis

Inter-model Variance



$$\delta P = \delta E + \delta DY + \delta TH + \delta NL + Res;$$

$$\delta TH = -(\langle \bar{\omega} \partial_p \delta \bar{q} \rangle + \langle \bar{v} \cdot \nabla \delta \bar{q} \rangle);$$

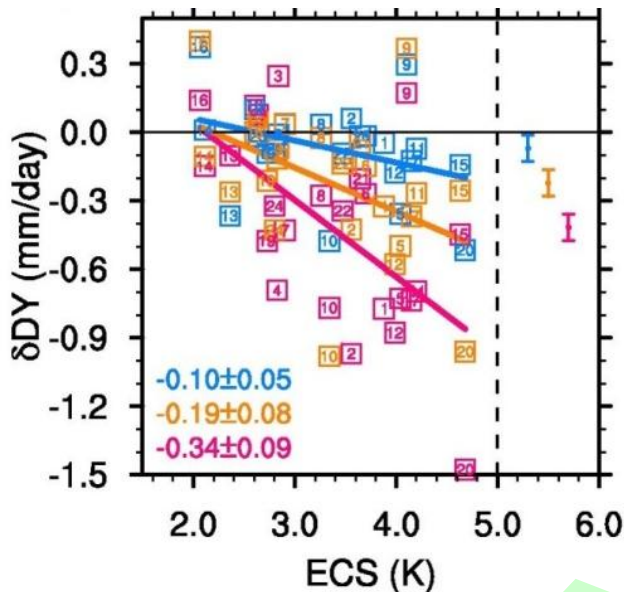
$$\delta DY = -(\langle \delta \bar{\omega} \partial_p \bar{q} \rangle + \langle \delta \bar{v} \cdot \nabla \bar{q} \rangle);$$

$$\delta NL = -(\delta \langle \overline{\omega' \partial_p q'} \rangle + \delta \langle \overline{v' \cdot \nabla q'} \rangle).$$

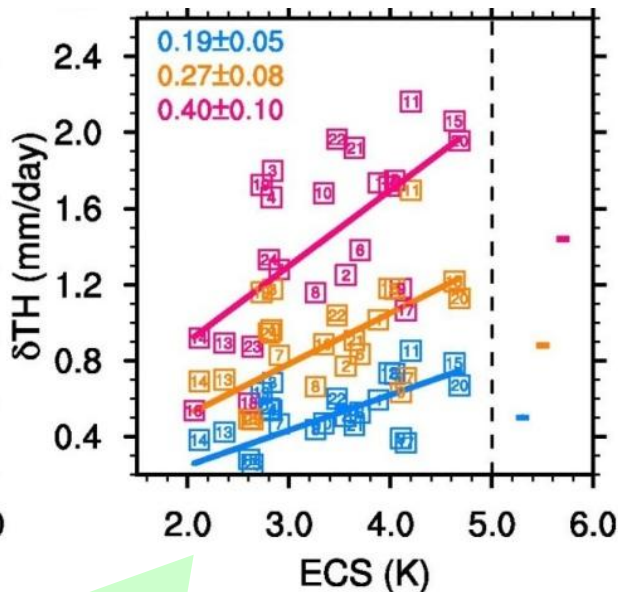
Rainfall Uncertainty — Moisture Budget Diagnosis



Dynamic



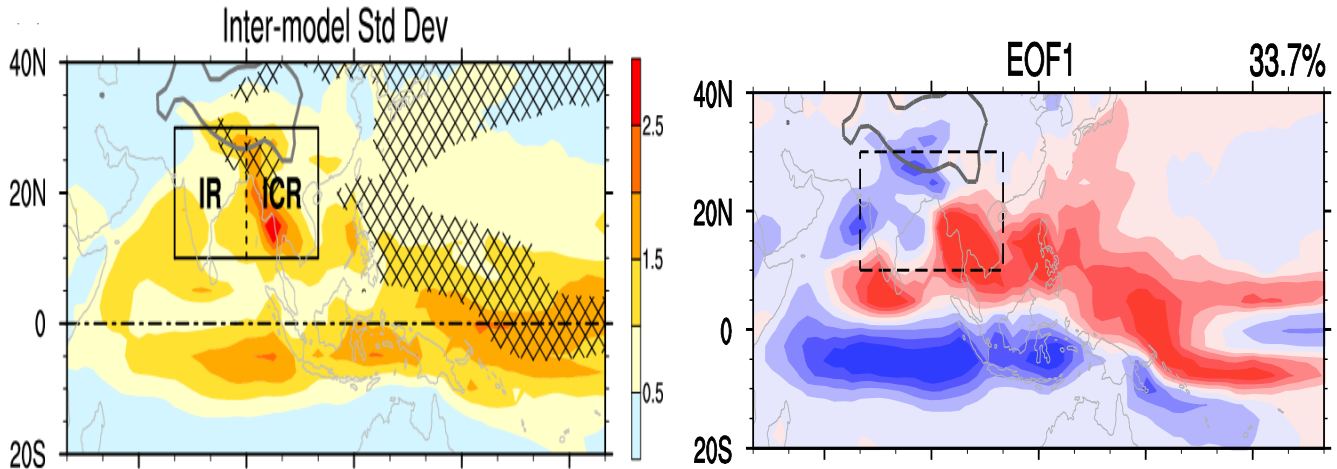
Thermodynamic



The offset between two terms: Weaker circulation but more water vapor



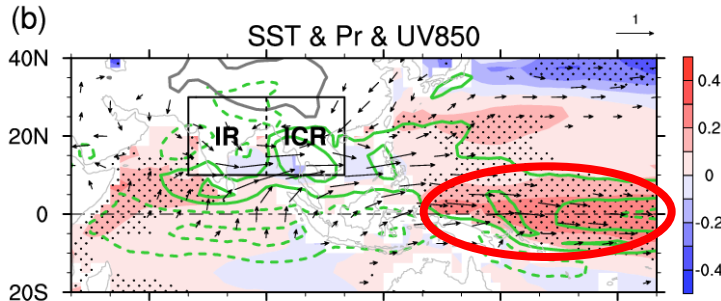
RCP85



Cross shading: signal larger than noise

Uncertainty mode: dipole between Indian region (IR) and Indo-China region (ICR)

Inter-model Anomalies regressed onto PC1

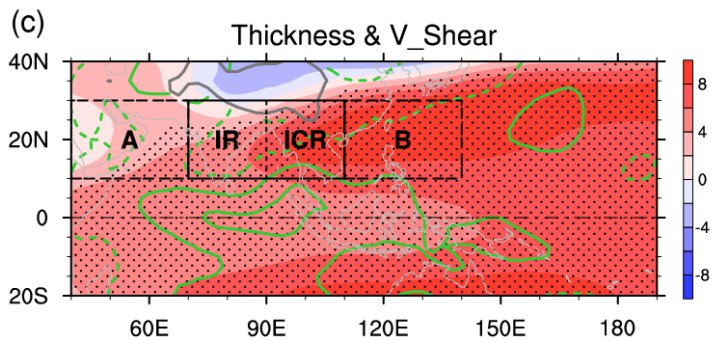


Shading: SST

Contour: Rainfall

Vector: 850hPa UV

Westerly anomalies as Lindzen-Nigam response



Shading: 500-200hPa Temp.

Contour: Vertical shear of meridional wind (Monsoon Hadley Circulation defined by Goswami et al. 1999)

Warmer SST in equatorial western Pacific

Stronger Convection

Descending over equatorial South Indian Ocean

Convergence of equator-crossing flow

Increasing ICR

Weaker zonal temperature gradient

Weaker monsoon Hadley circulation

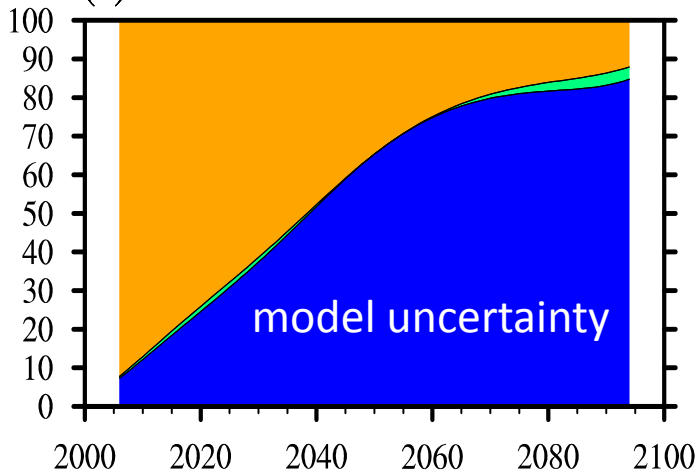
Decreasing IR



- ◆ Uncertainty in global mean warming (climate sensitivity) can explain most of the model spread in the projected SASM circulation except for the rainfall.
- ◆ Failure of global mean warming in scaling the regional rainfall spread is caused by equivalent effects of weakened circulation and increased moisture.
- ◆ The spread of SASM rainfall projection is resulted from the warming uncertainty in the equatorial western Pacific through modulating inter-hemispheric moisture transport and zonal temperature gradient over the SASM region.

Uncertainties in **E. Asian monsoon** projection

(b) East Asia



Model

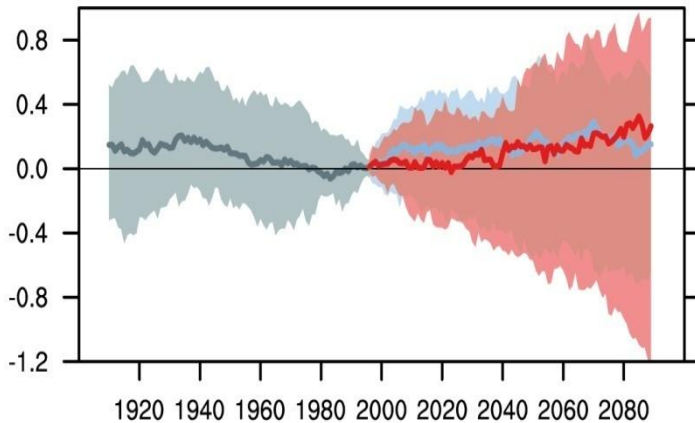
Scenario

Internal

Uncertainties
in E. Asian
summer monsoon
projection

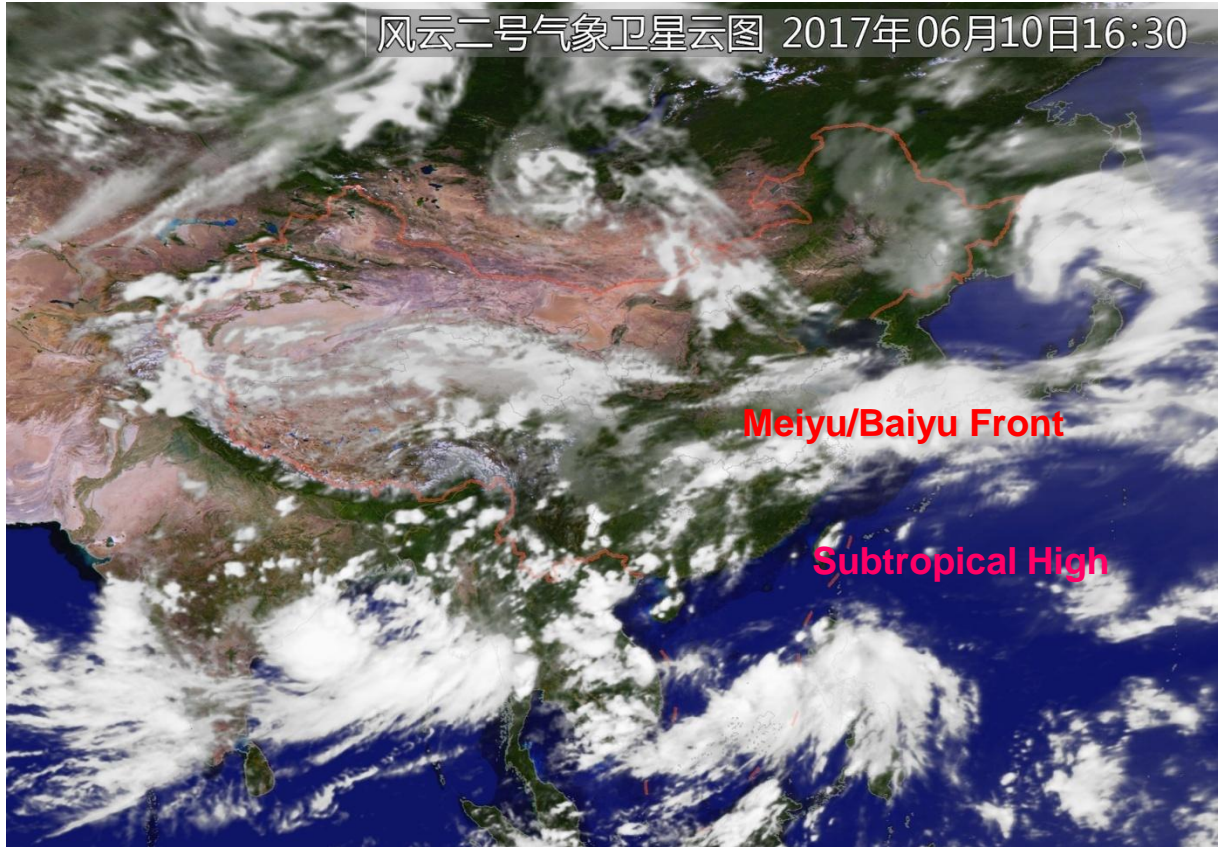
(a)

EAS





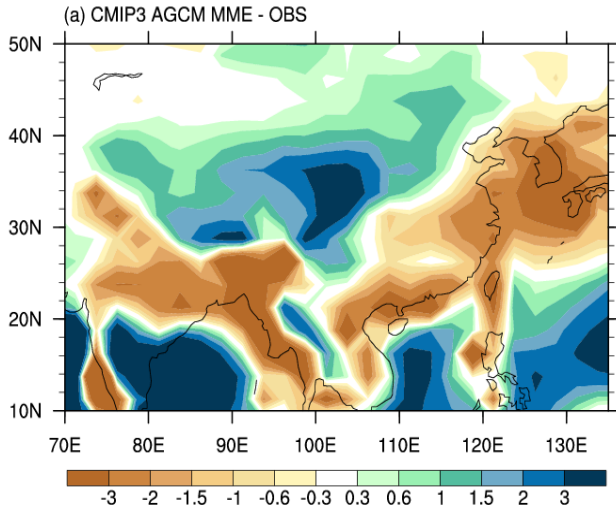
风云二号气象卫星云图 2017年06月10日16:30



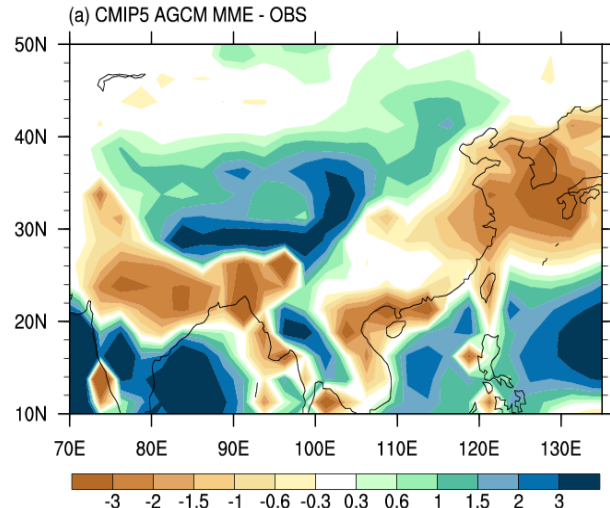
Challenges in the simulation of monsoon rain band



CMIP3

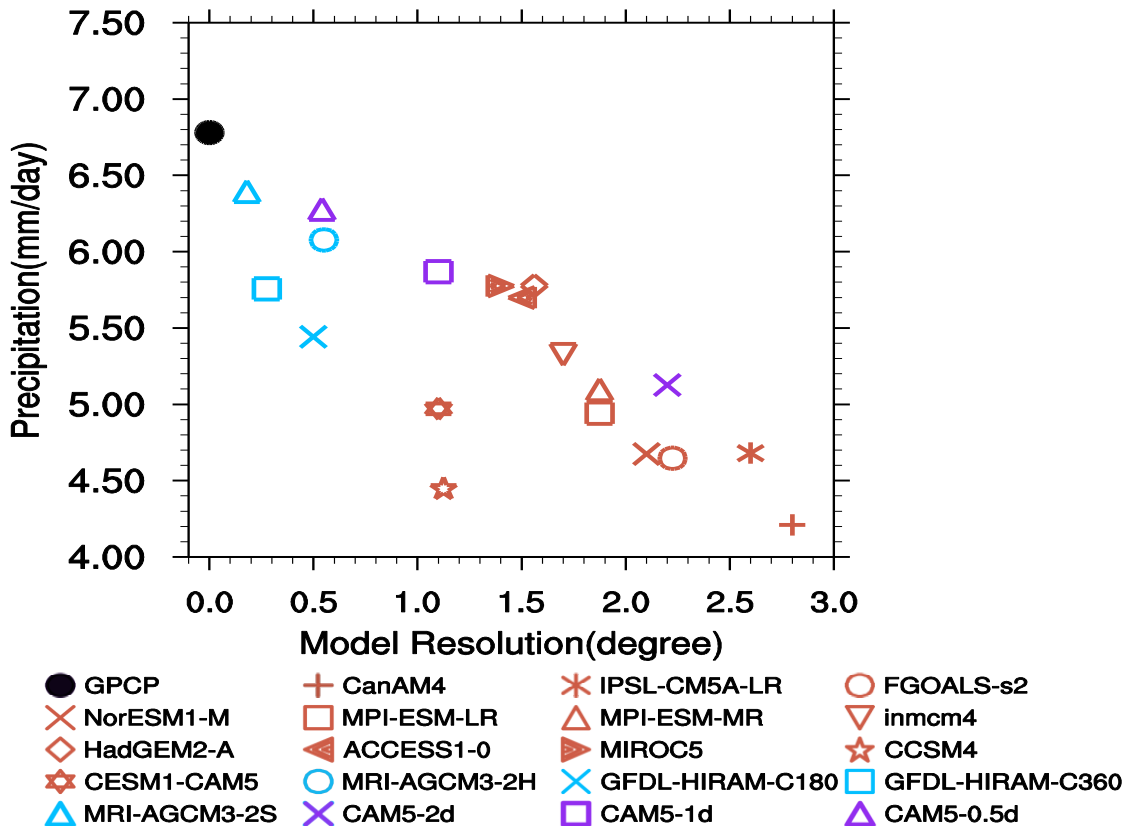


CMIP5



Mean state bias of JJA rainfall in CMIP3 & CMIP5 models

Monsoon (Meiyu) rainfall across the models



Moist Static Energy (MSE) budget analysis



$$\overline{\left\langle \frac{\partial M}{\partial t} \right\rangle} = \overline{F_{net}} - \overline{\langle v \cdot \nabla M \rangle} - \overline{\left\langle \omega \frac{\partial h}{\partial p} \right\rangle}$$

≈ 0

$\left\langle \frac{\partial h}{\partial p} \right\rangle$ Usually < 0 at deep convection area

thus where $\overline{\left\langle \omega \left(\frac{\partial h}{\partial p} \right) \right\rangle} > 0$ represent for ascending motion area

The left hand of upper equation usually ≈ 0 . Thus the right hand could be written as:

$$\overline{\left\langle \omega \frac{\partial h}{\partial p} \right\rangle} = \overline{F_{net}} - \overline{\langle v \cdot \nabla M \rangle}$$

The vertical motion can be estimated as the result of radiation and advection term.



$$\mathbf{X} = c_p T + L_v q \quad \mathbf{V} = (u, v)$$

$$\langle \overline{\mathbf{v} \cdot \nabla X} \rangle = \langle \overline{[\mathbf{v}] \cdot [\nabla X]} \rangle + \langle \overline{[\mathbf{v}] \cdot \nabla X^*} \rangle + \langle \overline{\mathbf{v}^* \cdot [\nabla X]} \rangle + \langle \overline{\mathbf{v}^* \cdot \nabla X^*} \rangle + \langle \overline{\mathbf{v}' \cdot \nabla X'} \rangle$$

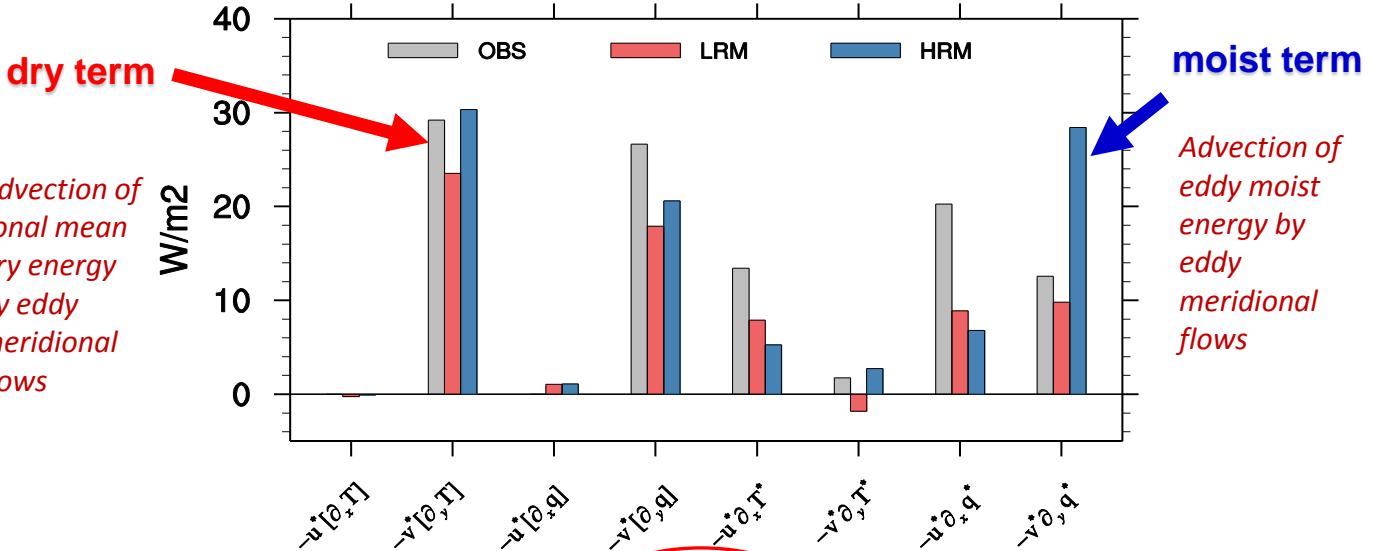
- Pure zonal mean moist enthalpy advection (small magnitude)
- **Advection of stationary eddy energy by the zonal-mean flow**
- **Advection of zonal-mean energy by eddy flow**
- Pure stationary eddy term
- Pure transient term

X' denotes the deviation from time \bar{X} (two-month June and July mean for each individual year), and X^* denotes the deviation from the global zonal mean $[X]$. T and q are listed as energy units.

Eddy flow: deviation from the global zonal mean

Decomposition of total horizontal moist enthalpy advection term

Decomposition



dry term

moist term

Advection of zonal mean dry energy by eddy meridional flows

Advection of eddy moist energy by eddy meridional flows

Zonal mean energy by eddy flow

$$\langle \overline{\mathbf{v}^* \cdot [\nabla M]} \rangle = \langle \overline{u^* \cdot [\partial_x T]} \rangle + \langle \overline{v^* \cdot [\partial_y T]} \rangle + \langle \overline{u^* \cdot [\partial_x q]} \rangle + \langle \overline{v^* \cdot [\partial_y q]} \rangle$$

Pure eddy advection

$$\langle \overline{\mathbf{v}^* \cdot \nabla M^*} \rangle = \langle \overline{u^* \cdot \partial_x T^*} \rangle + \langle \overline{v^* \cdot \partial_y T^*} \rangle + \langle \overline{u^* \cdot \partial_x q^*} \rangle + \langle \overline{v^* \cdot \partial_y q^*} \rangle$$

Averaged over the enhanced rainfall region (25°~ 34°N, 120°~ 155°E; units: W/m²). Each variable is vertically integrated. The observation is the mean of ERA-interim and JRA55.

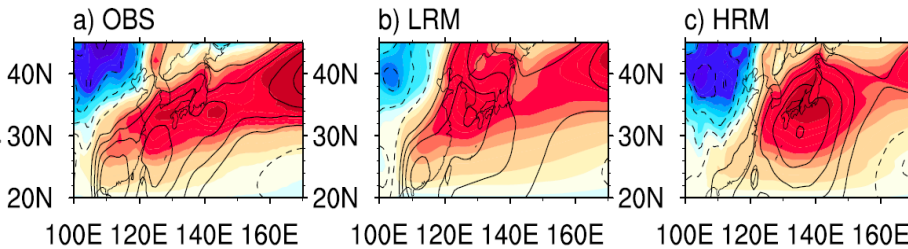
Dry term versus Moist term



Shading

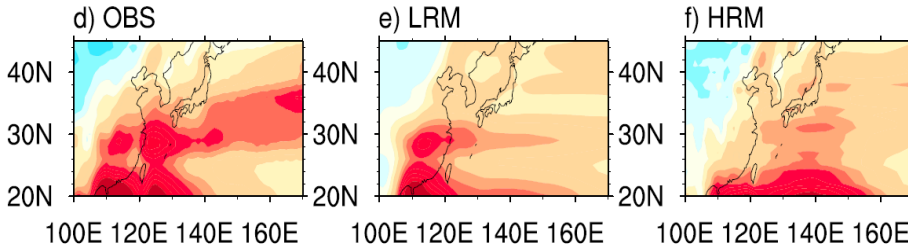
Contours

$-\langle \overline{v^* \cdot [\partial_y T]} \rangle$
dry term

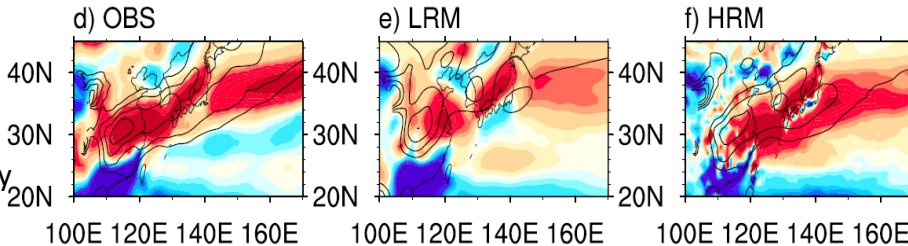


$\langle \overline{v^*} \rangle$

$-\langle \overline{v^* \cdot \partial_y q^*} \rangle$
moist term



$-\langle \overline{\partial_y q^*} \rangle$
meridional eddy
specific
humidity
gradient

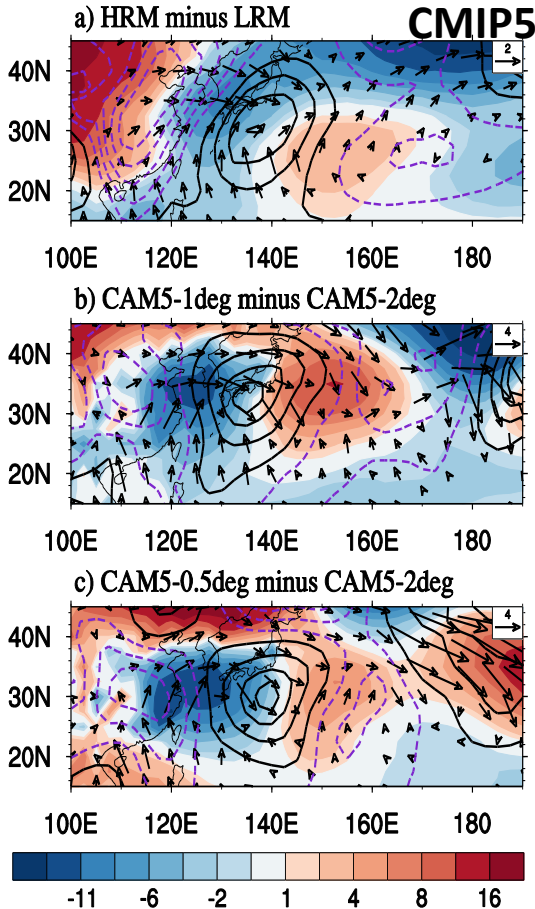


$\overline{\partial_y v^*}$ at 700 hPa



The enhanced energy transport along the MB rain belt in the HRMs is resulted from the enhanced meridional eddy velocity and its convergence in the HRMs

Sensitivity Experiments: Mechanisms



500 hPa

Shaded: geopotential height

Contour: meridional eddy velocity

Vector: wave activity flux

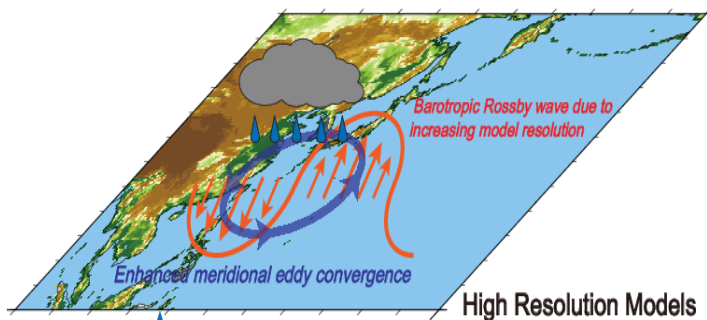
The differences of Z_g and v^* between HRMs and LRMs.

◆ Rossby wave like pattern generated downstream of Tibetan Plateau.

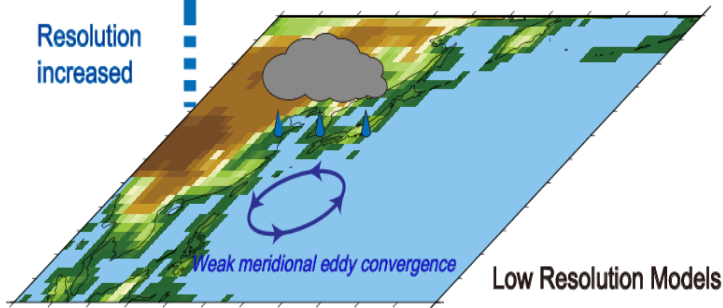
◆ WAFs transport eastward from Tibetan Plateau to far east of North Pacific ocean.

Schematic of the mechanism for the improvement of high-resolution models

Enhanced and reasonably reproduced rainfall



Weakened and northward shifted rainfall



- Due to increasing model resolution, a barotropic Rossby wave like response downstream of the Tibetan Plateau is generated.
- It further intensifies meridional convergence and moisture convergence along the EASM rain belt.
- Thus, the EASM rain belt is improved in the high-resolution models.

Implications?

Potential underestimation of future monsoon rainfall with CMIP5 models



Dependence of rainfall projection on model resolution

HadGEM3-GC2

RCP4.5

RCP8.5

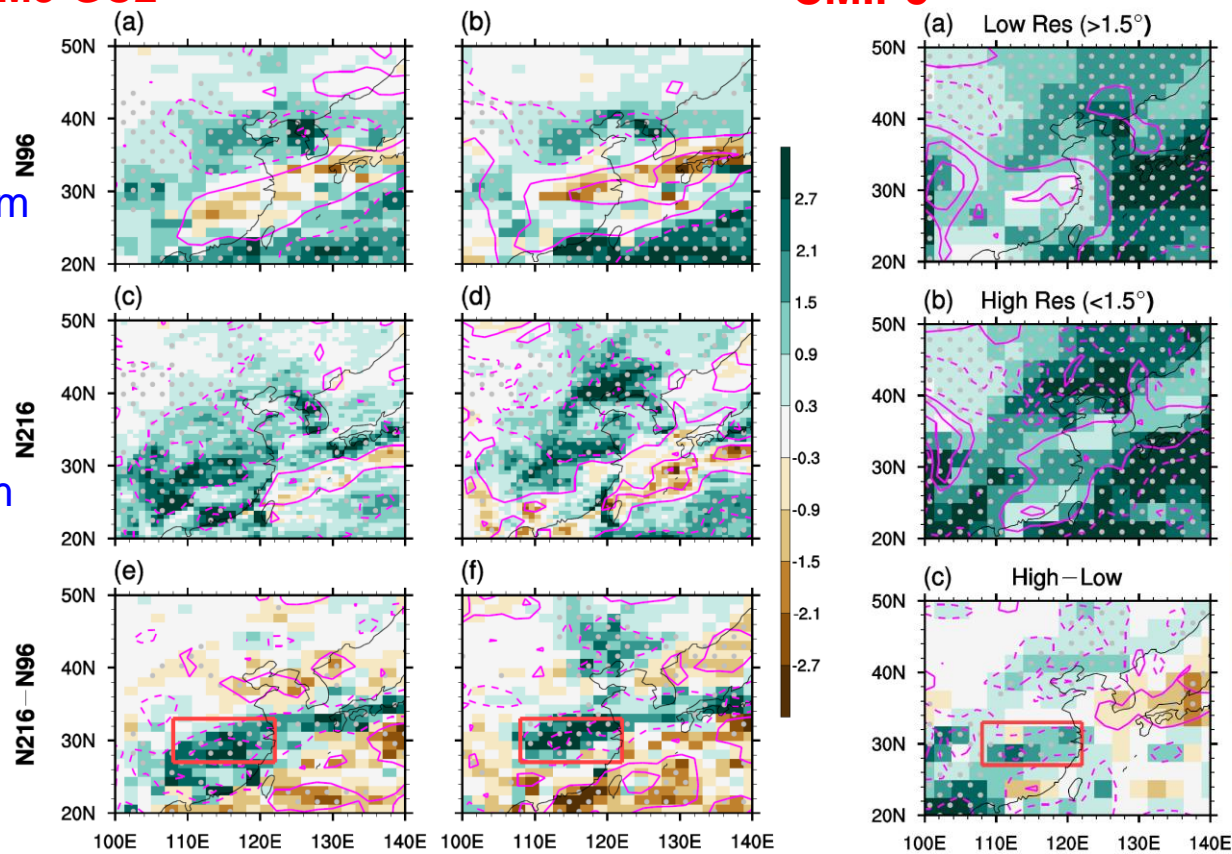
CMIP5

CMIP5 (RCP8.5)

~130km

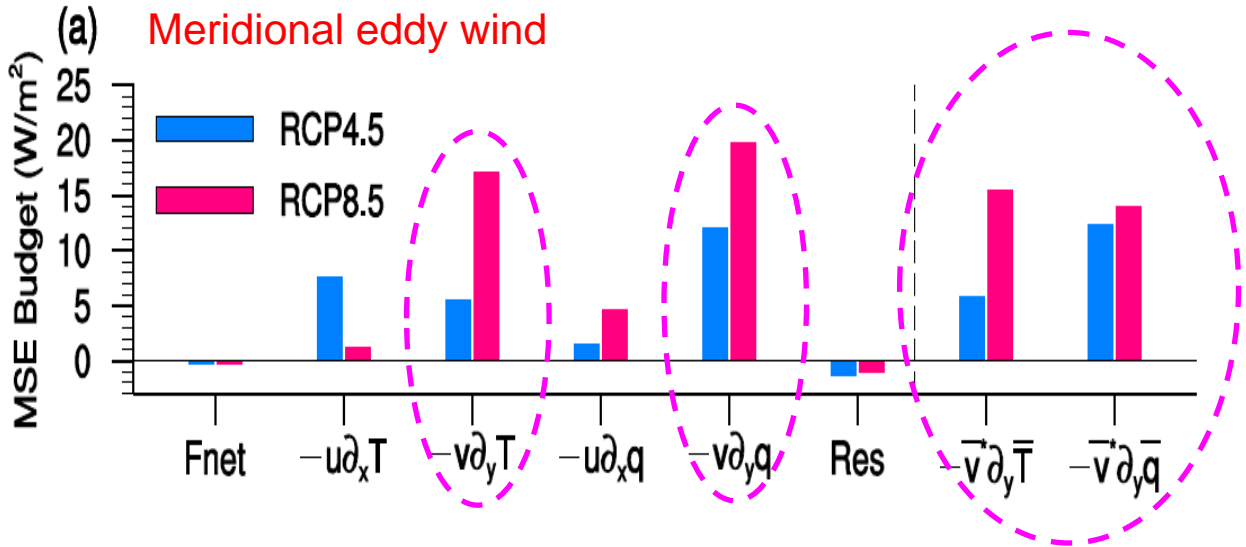
~60km

N216-
N96





Difference between N216 and N96 projection: MSE Diagnosis



$$\langle \omega \partial_p h \rangle = \overline{F_{\text{net}}} - C_p \overline{\langle \mathbf{V} \cdot \nabla T \rangle} - L_v \overline{\langle \mathbf{V} \cdot \nabla q \rangle}$$

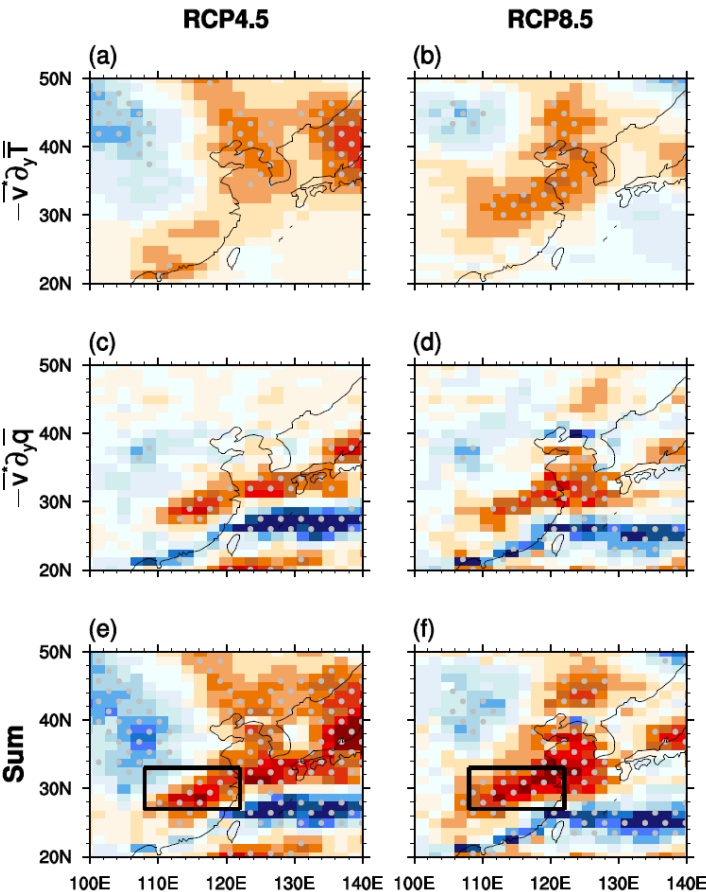
$$h = c_p T + L_v q + gz$$

h always increases with height.

$\langle \omega \partial_p h \rangle > 0$ means upward motion



Difference between N216 and N96 projection: MSE Diagnosis



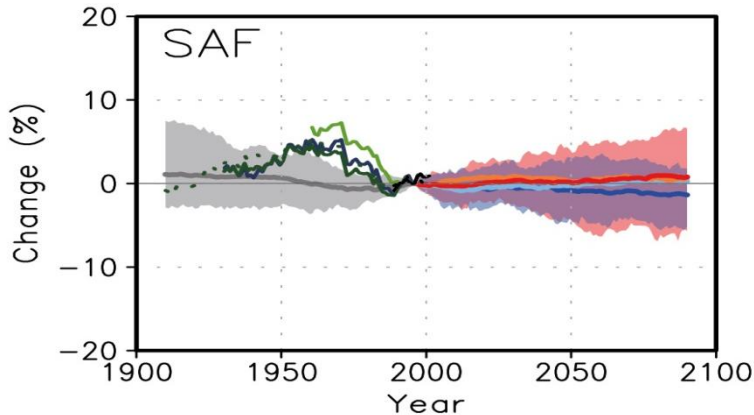
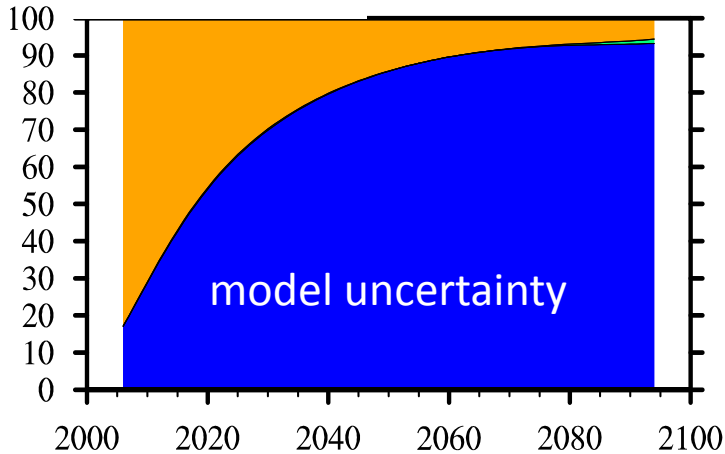
Meridional eddy wind
advects climatological
temperature and moisture
to the Meiyu front

$$-\bar{v}^* \partial_y \bar{T} \ \& \ -\bar{v}^* \partial_y \bar{q}$$



- A Rossby wave like response to realistic orography of the Tibetan Plateau helps to improve the simulation of monsoon rainband over East Asia.
- The projections of E. Asian summer monsoon rainfall has been underestimated by CMIP5 models.
- A higher resolution is favorable for transporting more moisture to the monsoon front region, thus increasing the projected rainfall over there.

SAF



Implication for the
projection of African
rainfall

Record-breaking climate extremes in Africa under stabilized 1.5 °C and 2 °C global warming scenarios

Shingirai Nangombe^{1,2,3}, Tianjun Zhou^{1,2*}, Wenxia Zhang^{1,2}, Bo Wu¹, Shuai Hu^{1,2}, Liwei Zou¹ and Donghuan Li^{1,2}

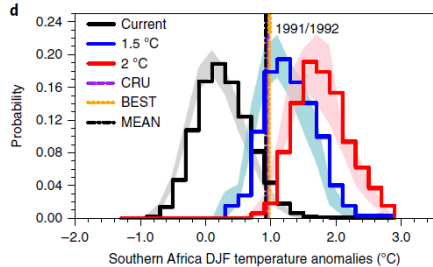
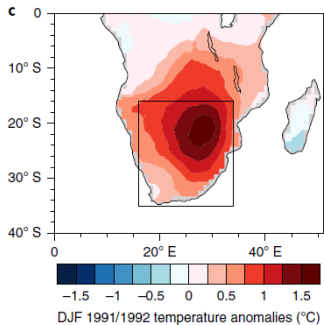
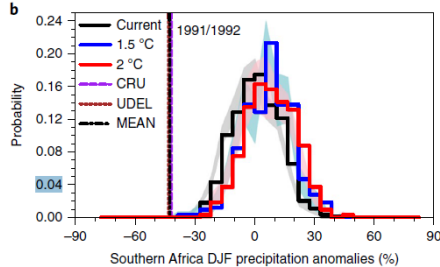
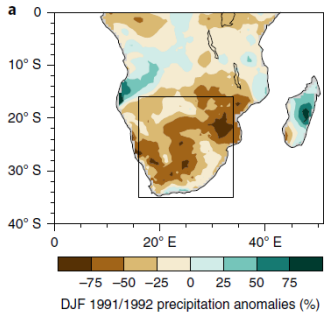
- **Model data:** CESM low warming experiments monthly data
- **Extreme events:** historical record-breaking climate events examined are:
 - (1) Extremely hot 2015 over Africa
 - (2) Extremely hot DJF 2009/2010 in North Africa
 - (3) Extremely high February 2000 precipitation over southeast Africa
 - (4) Severe drought of 1991/92 over southern Africa

✓ Baseline period of 1976 -2005 is referred to as the present day.

✓ The pre-industrial period in this study is 1850-1920.

✓ A period of 2071-2100 represents for the 1.5° C and 2° C warming period relative to pre-industrial levels.

1991/92 Southern Africa drought

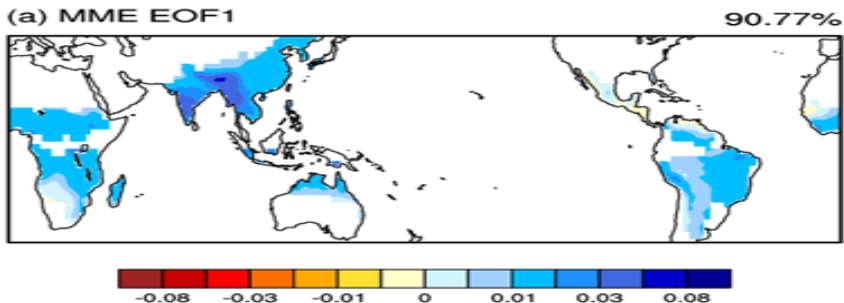


- Ts and Pr used as proxies for drought
- **1991/92 DJF extreme low precipitation over southern Africa**
 - projected to be rare in future scenarios
 - Consistent with the multi-model projections in CMIP5 over same area
- **1991/92 DJF extreme high temperature over southern Africa**
 - 1.5°C: **74%** (70%-78%)
 - 2°C: **98%** (97%-100%)

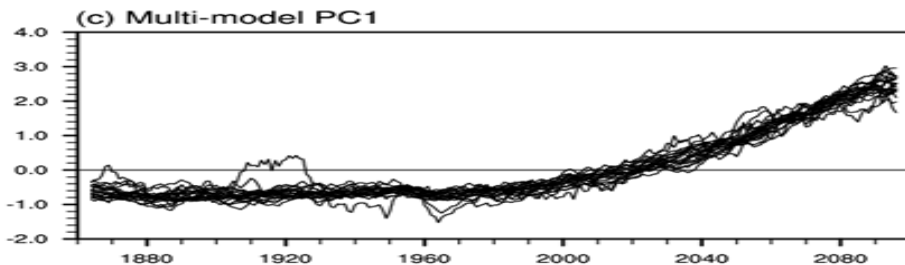
Regardless of the insignificant precipitation change projected, excessive warming alone might increase the probability of similar droughts occurring in warmer worlds

Extreme rainfall projection

The leading EOF of RX5day in CMIP5 RCP8.5 Projection



Increasing trend is evident in global monsoon domains except for N. American monsoon



Data: daily precipitation from 27 CMIP5 models: *historical* + *RCP4.5/RCP8.5*

The Goal of Paris Climate Agreement

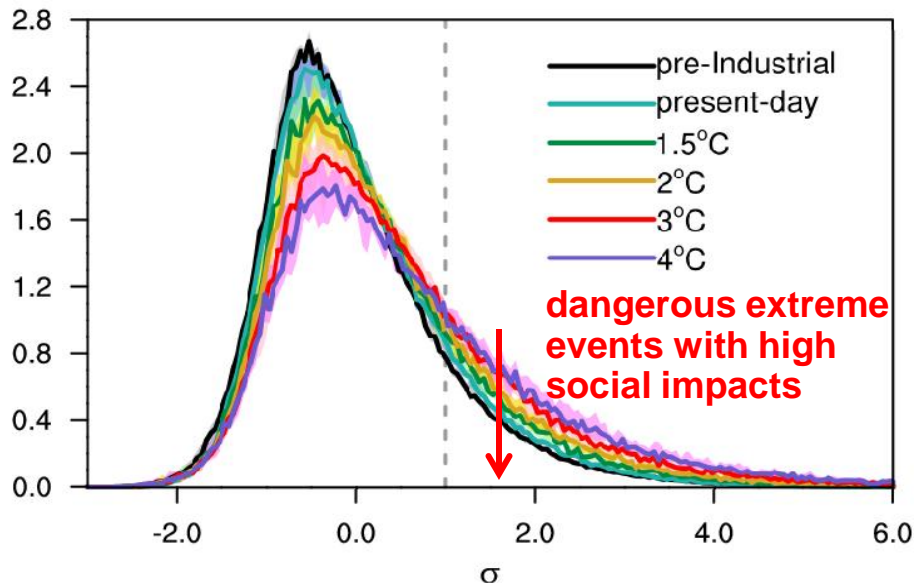
“Holding the increase in the global average temperature to well below 2°C above pre-industrial levels and pursuing efforts to limit the temperature increase to 1.5°C, recognizing that this would significantly reduce the risks and impacts of climate change”.



What are the reduced exposure to extreme precipitation in 0.5° C less warming?

Response of extreme precipitation to warming in CMIP5 Models

PDF of Rx5day over global land monsoon region



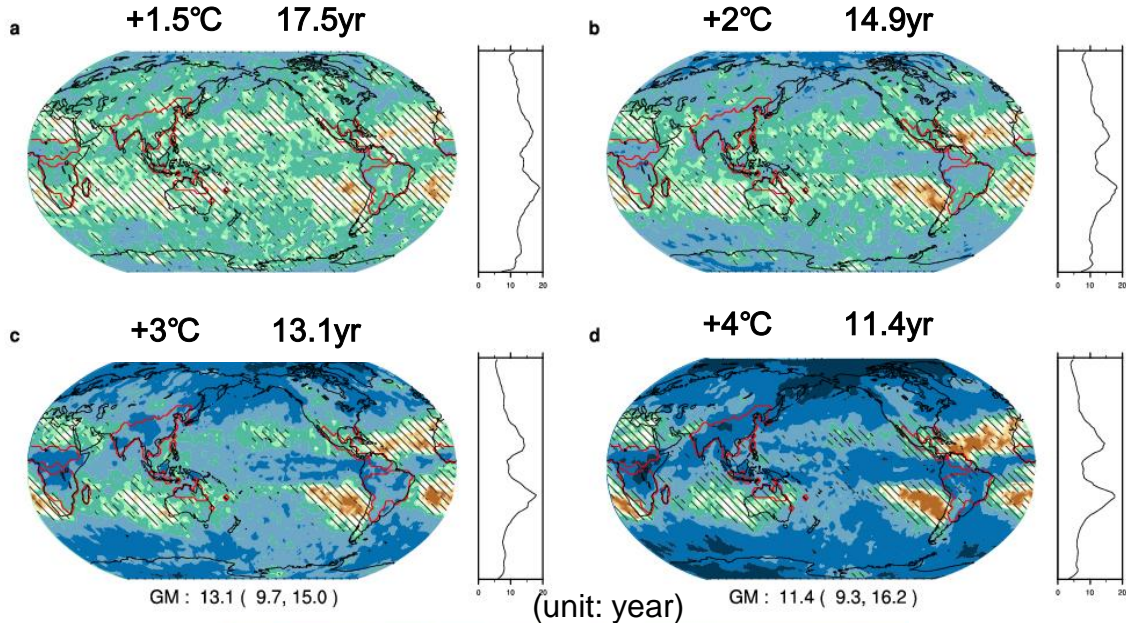
Once-in-10/20-year events
derived from Generalized
Extreme Value (GEV)
distribution

Two-folded response of extreme precipitation

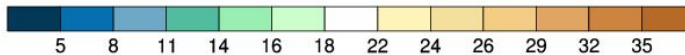
- Increase in mean state (shift of the distribution)
- Increase in variability (widening of the distribution)

Changes in return periods under warming conditions

Return periods of historical (1950-2005) *once-in-20-year* Rx5day events



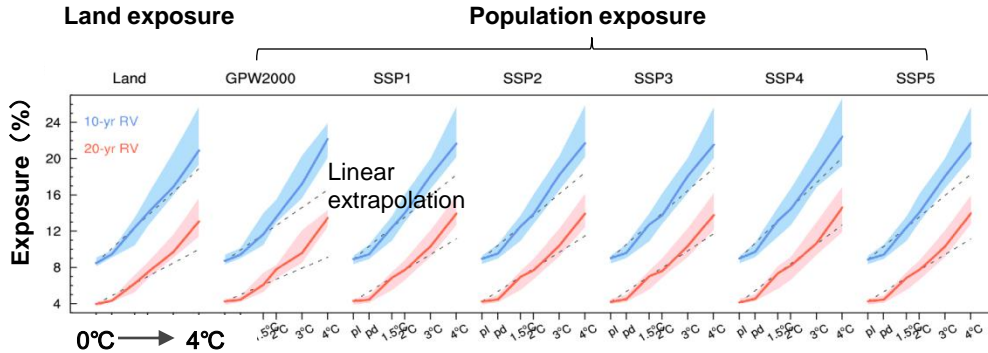
shorter return period



longer return period

Shorter return periods for dangerous extremes are expected under further warming conditions.

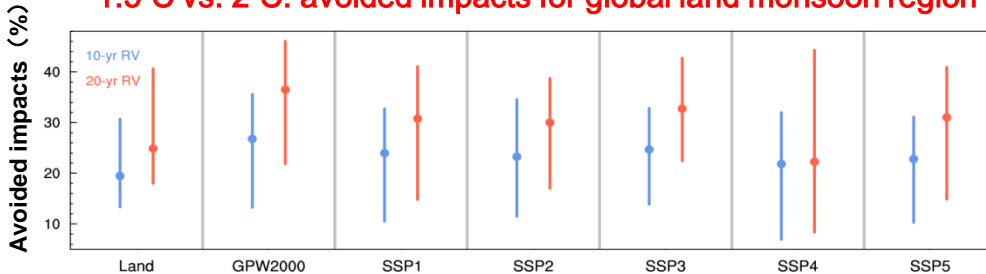
Increases in exposure with global warming levels



once-in-10-year events
once-in-20-year events

- Consistent increases in exposure to dangerous extremes with warming
- Nonlinear increases for warming higher than 2°C

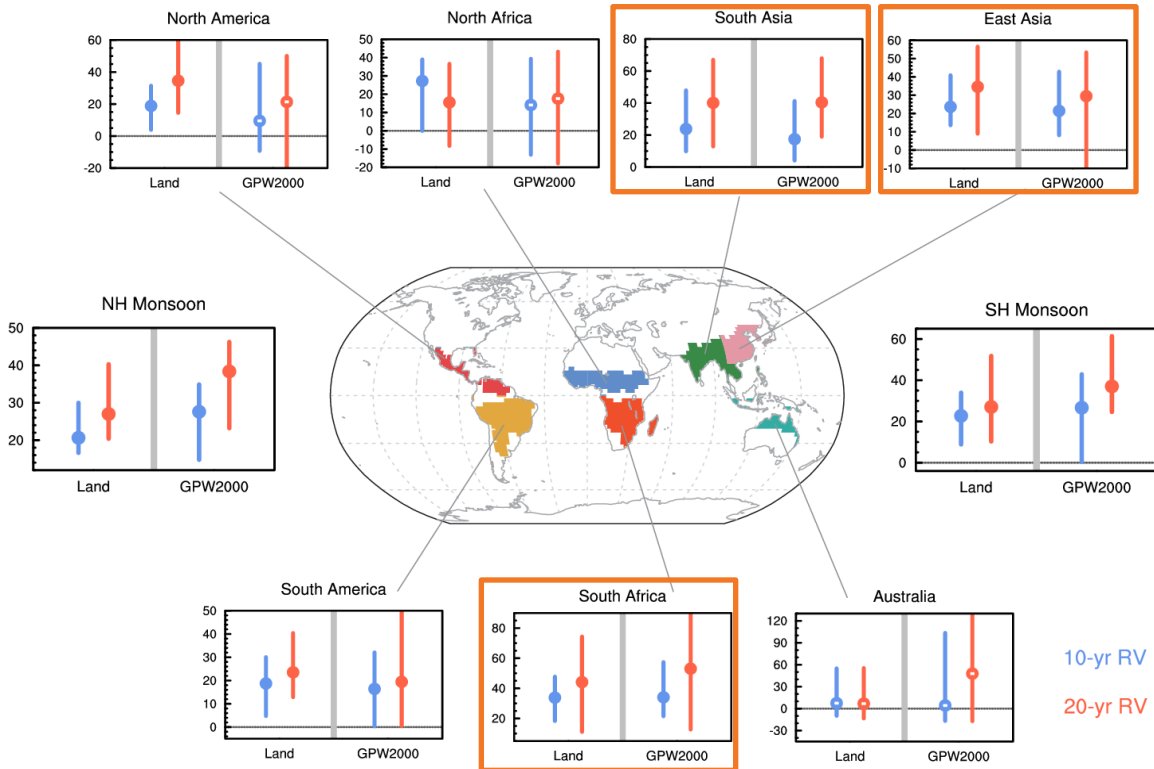
1.5°C vs. 2°C: avoided impacts for global land monsoon region



- Avoided exposure: ~20-40%
- More remarkable avoided impacts for more intense extremes

$$\text{Avoided Impact} = \frac{EXP_{2^{\circ}C} - EXP_{1.5^{\circ}C}}{EXP_{\text{present-day}}} \times 100\%$$

Avoided impacts: regional hotspots



◆ **South African, South Asian, and East Asian monsoon regions would benefit most from the 0.5° C less warming.**

Interim Summary 3



1. Both the mean state and variability of extreme precipitation would increase with warming, corresponding to the rightward shift and widening of the PDF, respectively.
2. Shorter return periods for dangerous extremes are expected under warming conditions, leading to increases in both areal and population exposures to dangerous extremes.
3. The 0.5° C less warming would reduce areal and population exposures to dangerous extreme precipitation (once-in-10/20-year) events by $\sim 20\text{-}40\%$, for the global land monsoon region.
4. South African, South Asian, and East Asian monsoon regions would benefit most from the 1.5° C low warming target, in terms of reduced exposure to dangerous extremes.

We highlights the benefits of the 1.5° C low warming target in terms of lower exposure to dangerous precipitation extremes for the populous monsoon regions.

Taking home messages



- ◆ *Projected changes of global land monsoon rainfall do not scale with global mean surface temperature.*
- ◆ *SST gradient associated with ECS can dominate regional patterns.*
- ◆ *High resolution is needed for the projection of monsoon rainfall.*
- ◆ *Limiting global warming to 1.5°C instead of 2.0°C would reduce exposures to precipitation extremes in global land monsoon domain.*